Data-based control synthesis and performance assessment for moored wave energy conversion systems: the PeWEC case

Data-based control synthesis and performance assessment for moored wave energy conversion systems: the PeWEC case

B. Paduano, F. Carapellese, E. Pasta, S. Sirigu, N. Faedo, and G. Mattiazzo

***Abstract*—With a model-based control strategy, the effectiveness of the associated control action depends on the availability of a *representative* control-oriented model. In the case of floating offshore wave energy converters (WECs), the device response depends upon the interaction between mooring system, any mechanical parts, and the hydrodynamics of the floating body. This study proposes an approach to synthesise WEC controllers under the effect of mooring forces building a representative data-based linear model able to include any relevant dynamics. Moreover, the procedure is tested on the moored pendulum wave energy converter (PeWEC) by means of a high-fidelity mooring solver, OrcaFlex (OF). In particular, the control action is computed with and without knowledge of the mooring influence, in order to analyse and elucidate the effect of the station-keeping system on the harvested energy. The performance assessment of the device is achieved by evaluating device power on the resource scatter characterising Pantelleria, Italy. The results show the relevance of the mooring dynamics on the device response and final set of control parameters and, hence, a significant influence of the station-keeping system on control synthesis and extracted mechanical power.**

***Index Terms*—Wave energy conversion, WEC, PeWEC, performance assessment, mooring system, control synthesis, OrcaFlex, nonlinear dynamics.**

I. Introduction

The pathway for sustainable energy transition has been strongly supported by United Nations by means of the sustainable development goals (SDGs) which aim, by 2030, to reach a significant spread of renewable energies [1]. In the current renewable technologies panorama, wave energy converters (WECs) represent a remarkable potential, being able to harvest energy from waves, which represent a substantial part of the total energy resource available in the oceans [2], [3].

Since the energy stored in a wave reduces as a function of the water depth and, clearly, the distance from shore [4], the majority of the proposed wave energy systems can be classified as offshore, floating devices [5], meaning that these WECs need to be confined in specific locations. As such, a vital component, which guarantees the proper functioning of such devices, is the mooring system, which is responsible of solving the station-keeping problem. Compared to traditional offshore structures (*e.g.* floating production storage and offloading units, among others) wave energy technologies represent more 'tangled' systems to station-keep, since the withstanding capability should not impact negatively in the energy extraction characteristics of the device.

Moreover, the extracted energy is commonly maximised adopting suitable control techniques, which stem from so-called optimal control theory. Bearing in mind that wave energy systems are generally controlled by means of an action computed by adopting a model-based approach, the effect of the mooring on the overall system response can play an important role in control synthesis, since the controller needs to be designed by means of a reliable model, including sufficient knowledge of any relevant dynamics. Furthermore, moorings can potentially exhibit a strongly nonlinear behaviour [6], and a rigorous inclusion of the significant dynamics within a tractable WEC model is, naturally, not straightforward. Although the influence of the mooring on device dynamics is a known problem in the current literature, the vast majority of the studies in the state-of-the-art wave energy panorama investigate mooring system design only for the case of survivability conditions, such as [7], [8], [9], just to cite a few.

The influence of the mooring system (analysed by means of a linear data-based model) on the device dynamics is discussed in [10], [11], which investigate the response of a generic floating body and the associated energy harvested, by leveraging a frequency-domain approach. Nonlinearities are included in the performance assessment of a moored wave energy system in [12], [13], where a pitching device is considered. Finally, Gubesch et al. [14] analyse the experimental response of an oscillating water column system in fixed conditions, moored by a taut and a catenary mooring system, reporting a significant reduction on device performance. Nonetheless, apart from the analysis in [15] (which considers the experimental characterisation of a moored device for control purposes), control design/synthesis for WECs is always performed *without* including the influence of the mooring systems, even though these can have a strong influence on power production and overall dynamics, as discussed within this section.

Motivated by the influence of the mooring systems in both energy-maximising WEC control synthesis, and corresponding performance assessment, this study proposes a control-oriented data-based modelling procedure to include the mooring relevant dynamics, and perform a controller synthesis by means of the impedance-matching technique [16]. The data-based structure is computed based on the system identification procedure proposed, and the resulting characterisation is leveraged for the computation of the corresponding control parameters via the impedance-matching principle. In order to include any relevant

The authors are with the Mechanical and Aerospace Department (DIMEAS), Politecnico di Torino, Turin, Italy (e-mail: bruno.paduano@polito.it).

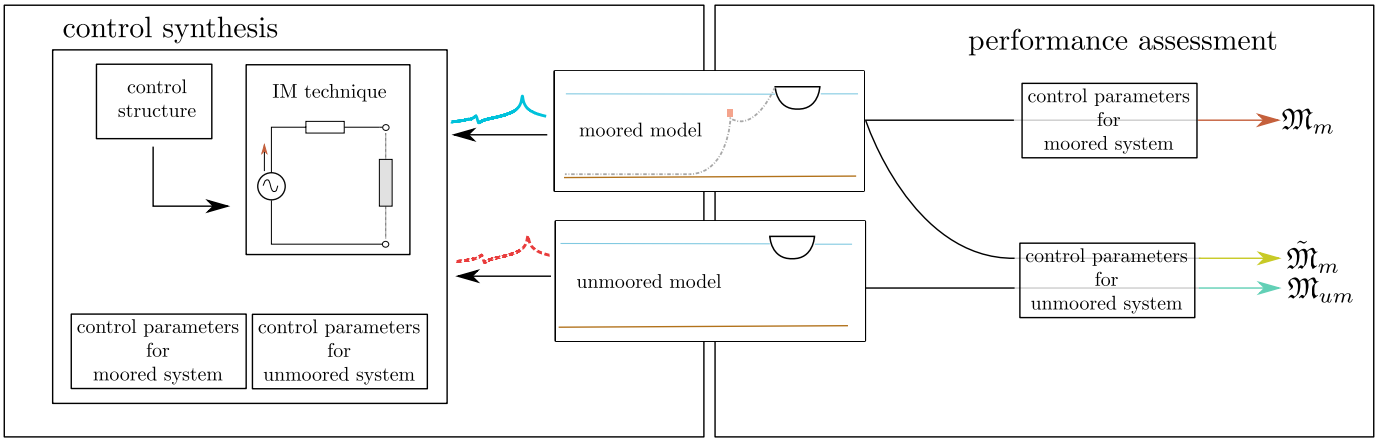

Fig. 1. Mooring influence on the extracted energy - workflow. On the left-hand side of the picture, the control synthesis is achieved by indentifying the moored and unmoored responses, and by leveraging the impedance-matching principle. Consequently, on the right-hand side, the device performances are evaluated in different scenarios, *i.e.* ignoring the mooring dynamics when synthesising the associated controller ($\tilde{\mathfrak{M}}_m$), including mooring dynamics in control synthesis ($\mathfrak{M}_m$), and by considering a fully unmoored model ($\mathfrak{M}_{um}$).

mooring-related dynamics, the target data, used to compute such data-based control-oriented representation, is generated with a high-fidelity modelling solver, by using a specific set of representative persistenly exciting inputs. Among the several models available for mooring dynamics, ORCAFLEX (OF), a dynamic lumped-mass model [17], is adopted within this study, for its reliability and wide-use within the renewable offshore field [17]. Moreover, given that OF is not able to evaluate the associated WEC extracted power (and simply provides a solution for the mooring dynamics), the integration of both the electro-mechanical part associated with any realistic WEC, and corresponding controller implementation, is achieved by compiling a dynamic library from a Simulink nonlinear model. The proposed integration procedure can be easily generalised for the inclusion of any external force/interaction in OF, representing a powerful tool, considering the wide use of this software in a vast number of marine applications.

Finally, by applying the outlined procedure to a relevant case-of-study, this manuscript eviscerates the several aspects related to the influence of the mooring on harvested energy, in order to expose the effect of the station-keeping system on device dynamics and associated control synthesis procedure. The performance assessment is evaluated picking several environmental conditions on a scatter diagram of a specific site, to respect both a real sea state condition, and a representative set of wave periods and heights to characterise the device response in the light of the model nonlinearities. The WEC under investigation is the *pendulum wave energy converter* (PeWEC) [18]. The PeWEC has been selected as case-of-study for a number of reasons, including its multi-degree-of-freedom (DoF) nature, comprehensive PTO conversion mechanism, and relevance of the mooring system for device station-keeping and aligment, being a representative case for the analysis of the proposed methodology.

The analysis presented in this paper can be divided in two main parts:

- In the first part, a *general* approach to achieve energy-maximising control synthesis of a moored system is proposed, by leveraging results from impedance-matching theory [16]. The corresponding mooring dynamics, and any nonlinear 'external' actions, are identified and included within a representative data-based model, which is adopted for the computation of a representative control action. This part is schematically described in the left-hand side of Figure 1 where, by means of a data-based model, the control parameters are synthesised with and without the inclusion of the relevant mooring dynamics.
- Within the second part, the PeWEC case is presented. The proposed methodology is applied to the PeWEC system and, consequently, its associated performance assessment is evaluated on a representative set of waves. In particular, the control synthesis is achieved for both moored, and unmoored conditions. The performance assessment is then performed considering a wave scatter corresponding with the island of Pantelleria (Sicily, Italy). The energy harvested with the moored device is evaluated by using the control parameters computed for both moored and unmoored conditions (and the associated scenarios are referred to as $\tilde{\mathfrak{M}}_m$ and $\mathfrak{M}_m$, respectively), in order to evaluate the influence of the mooring system on the control design procedure. Furthermore, the investigation of the mooring influence on device dynamics and, hence, on harvested energy, is completed by comparing the results achieved for the moored system with a completely unmoored configuration (*i.e.* by analysing the response in the scenario $\mathfrak{M}_{um}$). This part is schematically described in the right-hand side of Figure 1.

The reminder of this article is structured as follows. Section I-A provides an account of the main notation used throughout this study. In Section II, the control synthesis procedure is proposed, and the methodology to characterise the corresponding data-based model is discussed. In Section III, the PeWEC case is presented. Section IV describes the numerical models adopted and the integration of any external action within the high-fidelity solver OF. Moreover, the proposed control synthesis approach is applied and discussed for PeWEC, in Sec-

tion V. Section VI describes the corresponding performance assessment for the PeWEC, considering the selected scatter diagram. Finally, Section VII outlines the main conclusions of this study.

Note that a preliminary version of this study has been presented in the conference paper [19]. The present study vastly extends [19] in the following sense:

(a) The methodology to achieve the control design of a moored WEC is defined and generalised to any WEC.
(b) Since OF is one of the most adopted software within the offshore renewable field, a procedure to include any external action and, hence, PTO action within its controller, is presented.
(c) The PeWEC case, is outlined on a real site representative set of waves, and the effectiveness of the control synthesis and the influence of the mooring on device dynamic is evaluated on the proposed sea states.

A. Notation

$\mathbb{R}^+ \subset \mathbb{R}$ denotes the set of non-negative real numbers. Time-domain forces/torques are denoted with calligraphic capital letters, *e.g.* $\mathcal{F}(t)$, while their corresponding Fourier transforms are denoted with upper-case letters, *i.e.* $\mathfrak{F}(\mathcal{F}(t))(\omega) \equiv F(\omega)$. Time-domain motion variables are denoted with lower-case letters, e.g. w, while their corresponding Fourier transform is consistently represented with upper-case letters, *i.e.* $\mathfrak{F}(w(t))(\omega) \equiv W(\omega)$. The Fourier transform of the variable $\dot{\epsilon}$ is indicated with $\dot{E}$. Given $z \in \mathbb{C}$, the notation z^* is used to denote its complex-conjugate, while $\Re(z)$ and $\Im(z)$ indicate the real- and imaginary-parts of z, respectively. Given a time-domain quantity $p(t)$, the notation $\overline{p(t)}$ indicates its mean value over a given set.

II. Control sythesis and control-oriented modelling

In this section, the considered energy-maximising control synthesis is introduced, and the procedure proposed for the computation of the corresponding control action is discussed. To keep this paper reasonably self-contained, a brief discussion of the general field of WEC control is presented in the following paragraphs, to highlight the main characteristics of the proposed procedure. A generic 1-DoF wave energy system

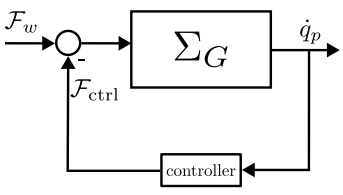

Fig. 2. Figure 2: Schematic representation of a generic SISO wave energy system.

can be described as exposed in Figure II, in which $\dot{q}_p : \mathbb{R}^+ \to \mathbb{R}, t \mapsto \dot{q}_p(t)$ is the device velocity, Σ_G is the WEC representative model (*i.e.* dynamical operator), which is feedback actuated by a corresponding energy-maximising controller and, finally, $\{\mathcal{F}_w, \mathcal{F}_{\text{ctrl}}\} : \mathbb{R}^+ \to \mathbb{R}, t \mapsto \{\mathcal{F}_w(t), \mathcal{F}_{\text{ctrl}}(t)\}$ are the excitation force (*e.g.* wave induced force) and control force, respectively. Within the marine energy field, control systems are commonly in charge of maximising the energy harvested from the source. In particular, the control procedure for WEC systems can be written in terms of an associated optimal control problem (OCP). Briefly summarising, the aim is to find a control action, $\mathcal{F}_{\text{ctrl}}$, such that:

$$\text{OCP}(\mathcal{F}_{\text{ctrl}}) : \begin{cases} \max\limits_{\mathcal{F}_{\text{ctrl}} \in \mathbb{R}} L(\mathcal{F}_{\text{ctrl}}), \\ \text{subject to:} \\ \dot{q}_p = \Sigma_G(\mathcal{F}_w - \mathcal{F}_{\text{ctrl}}), \end{cases} \tag{1}$$

where, $L(\mathcal{F}_{\text{ctrl}}) \in \mathbb{R}$ is the harvested energy from ocean waves, which can be defined, over a time interval $\Delta t = [t_1, t_2]$, as:

$$L(\mathcal{F}_{\text{ctrl}}) = \frac{1}{t_2 - t_1} \int_{\Delta t} \mathcal{F}_{\text{ctrl}}(t) \dot{q}_p(t) \mathrm{d}t, \tag{2}$$

The OCP in equation (1) depends upon the definition of a suitable model, representing the equality constraint related to device dynamics. Clearly, the model represents an approximation of the WEC dynamics, and the reliability of the computed control action is strictly related to the faithfulness of the model and its aptitude to approximate, with sufficient fidelity, all the relevant dynamics [20].

Within the wave energy field, the optimal control action, solution to the OCP (1), can be computed by means of several strategies, which can be divided into 2 main categories [21], namely impedance-matching based strategies, and optimisation-based strategies.

According to the family of optimisation-based controllers for WEC systems, the solution of the OCP (1) is approximated by leveraging numerical techniques, which are commonly classified in direct and indirect optimal control methods [22]. These methods transcribe the energy-maximising problem (*i.e.* OCP, (1)) into a nonlinear program (NP), to subsequently solve such a NP by means of numerical routines. Clearly, in the case of optimisation-based strategies, the associated control action needs to be synthesised and computed efficiently (in a computational sense). Among well-established techniques available for WECs, within this family, one can find *e.g.*[1] model predictive control (MPC) [23] and pseudo-spectral control [24][1].

The impedance-matching theory, discussed in Section II-A, represents the core of several control techniques, *e.g.* [26], and assumes availability of a representative linear model of the WEC dynamics. The main advantage of these techniques is that, in contrast to optimisation-based strategies, no numerical routine is required to compute the associated control action where, the use of numerical, computationally expensive, models can represent a bottleneck for the definition of the control action. In the light of this, a procedure to compute a representative linear model for the WEC dynamics is proposed within this section, based on input/output data generated with the high-fidelity mooring solver OF, following the discussion provided in Section II-B.

[1]For a complete dissertation please see [21], [25]

A. Impedance-matching-based control synthesis

Under linear modelling assumptions, the WEC dynamics can be described in terms of a linear time-invariant (LTI) system, as schematically represented within Figure 3, where $\{G, F, \dot{Q}_p\} : \mathbb{R} \to \mathbb{C}$ represent the input/output frequency response of the *controlled mode*[2] associated with the WEC system, the Fourier transform of the (total) mechanical system excitation force, and the controlled variable $\dot{Q}_p$, respectively (see [16]). Finally, $I_u^{\text{opt}} : \mathbb{R}^+ \to \mathbb{C}$ represents the controller frequency response.

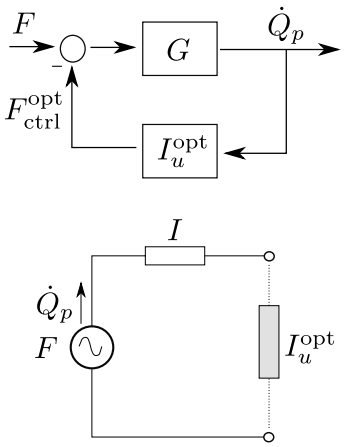

Fig. 3. System representation under LTI assumptions (top), and associated schematic representation of the electric-analogous (bottom). Adapted from [16].

The resolution of the energy-maximising control problem for WECs, leveraging the electrical representation in Figure 3, can be addressed by means of the so-called impedance-matching theorem [27]. This principle states that, to maximise power transfer from the source (*i.e.* the total mechanical system excitation force F) , the load impedance I_u needs to be designed as the complex-conjugate of the system impedance $I = G^{-1}$, that is, for the WEC case:

$$I_u^{\text{opt}} = I^* = G^{*-1}. \tag{3}$$

The equation of motion, under the condition derived in equation (3), becomes:

$$\begin{aligned} \dot{Q}_p &= G(F - F_{\text{ctrl}}^{\text{opt}}), \\ F_{\text{ctrl}}^{\text{opt}} &= G^{*-1}\dot{Q}_p, \end{aligned} \tag{4}$$

in which $F_{\text{ctrl}}^{\text{opt}} : \mathbb{R} \to \mathbb{C}, \omega \mapsto F_{\text{ctrl}}^{\text{opt}}$ is the optimal control action (derived in the frequency domain). Although the condition expressed in (3)-(4) is that effectively providing maximum energy absorption, the resulting associated optimal control action is *anti-causal*, due to the nature of the analytic continuation of the complex-conjugate operator to $\mathbb{C}$ (the reader is referred to [16] for further discussion on this issue). In other words, the condition in (3)-(4) cannot be directly implemented, though stable and causal structures can be used to approximate this condition accordingly, as further discussed within this section. We further note that, from conditions (3)-(4), energy-maximisation implies the following closed-loop frequency-response function:

$$W^{\text{opt}}(\omega) = \frac{G(\omega)G^*(\omega)}{G(\omega) + G^*(\omega)}, \tag{5}$$

in which $W^{\text{opt}} : \mathbb{R} \to \mathbb{R}^+, \omega \mapsto W^{\text{opt}}(\omega)$ works as an ideal, zero-phase filter, i.e. the response $\dot{Q}_p$ is in-phase with the force $F(\omega)$ in idealised energy-maximising conditions.

Since the implementation of the optimal controller structure, achieved by means of the application of the impedance-matching theorem, cannot be pursued for its associated non-causality (see the discussion immediately above), the integration of such methodology within a feedback controlled system can be achieved by approximating the optimal velocity-to-control force map with a suitable control structure [16]. In particular, we consider interpolation of the condition expressed in (3) at a particular (well-selected) frequency ω_i, *i.e.*

$$I_u(\omega_i) = I_u^{\text{opt}}(\omega_i). \tag{6}$$

The specific parametric structure for I_u, adopted within this manuscript, is motivated and described within Section V.

B. Data-based modelling

Following the impedance-matching approach presented in Section II-A, the procedure for the identification of a representative device frequency-response map $G(\omega)$, so as to effectively leverage the result in (3), is outlined below. We begin by noting that the optimal control frequency response is effectively influenced by any external force (see Figure 3) and associated mooring system, and hence these need to be included appropriately in G.

The identification of the frequency response $G(\omega)$ is achieved by suitable estimation of an associated empirical transfer function, imposing a set of known (sufficiently exciting) input signal via the control (PTO) $\tilde{\mathcal{F}}_{\text{ctrl}}$. Although several signals can be employed for the identification of the corresponding frequency response (see, for instance, [28]), a multisine signal is adopted within this paper, taking advantage of *e.g.* its periodicity and bounded spectrum [29].

In particular, the set of multisine signals is built by applying the so-called *Schroeder* phases [30]:

$$\begin{aligned} \tilde{\mathcal{F}}_{\text{ctrl}}^j(t) &= \sum_{k=1}^{N_k} a_j \cos(\omega_k t + \phi_k), \\ \phi_k &= \frac{-k(k+1)}{N_k}, \qquad \forall k \in \{1, \dots, N_k\}, \end{aligned} \tag{7}$$

where $a_j \in \mathscr{A} \subset \mathbb{R}^+$, $j \in \{1, \dots, N_j\}$, defines the final signal amplitude. Since the model to characterise in terms of a representative linear mapping G has, naturally, a nonlinear behaviour, the input signal $\tilde{\mathcal{F}}_{\text{ctrl}}$ needs to be tested under several amplitude conditions $a_j \in \mathscr{A}$.

Note that, only the controllable input $\tilde{\mathcal{F}}_{\text{ctrl}}$ is required herein to characterise the underlying system: In other words, F and F_{ctrl} act in a superposition fashion as a "unique" input to

[2]Note that the considered model G effectively describes the dynamics of the system 'projected' onto the controlled DoF, and not the full I/O dynamics of the WEC system (see the arguments posed in [16]).

the system G, *i.e.* $F - F_{\text{ctrl}}$. This effectively means that, for system identification procedures, the uncontrollable input F can be considered to be 0, and hence the system is excited by means of the controllable input F_{ctrl}, in order to characterise the input/output map G. This is effectively consistent with previous studies in system identification for WEC systems (see *e.g.* [11], [10]).

Using each input element in the set $\mathscr{A}$, and evaluating the associated DoF velocity $\dot{q}_p^j$, it is possible to construct the average empirical transfer function estimate as

$$G(\omega) = \sum_{j=1}^{N_j} \frac{1}{N_j} \frac{\dot{Q}_p^j(\omega)}{\tilde{F}_{\text{ctrl}}^j(\omega)}. \tag{8}$$

Please note that the exciting signal $F_{\text{ctrl}}^j(\omega)$ needs to be designed according to the system response, *i.e.*:

- The frequency bandwidth is chosen in order to excite any relevant dynamics.
- The signal (experiment) duration needs to be tuned accordingly, since it naturally relates, in periodic signals, to the frequency discretisation (*i.e.* the frequency discretisation needs to be small enough to characterise any relevant dynamic).
- The associated signal amplitudes are defined accordingly to the operating conditions. For example, in [11], the exciting signal is chosen to have the same energy as the wave frequency motion.

For further information, the reader is referred to *e.g.* [29].

Following the mooring-related WEC studies [11], we propose a methodology to compute a *representative* linear model for the moored WEC, valid for a given set of wave operating conditions for the device, *i.e.* significant wave heights and peak periods. To achieve this, we employ tools from the field of system identification, and we propose a methodology to provide representative models via so-called black-box structures, using only input-output data in the frequency-domain (also known as best linear approximation [31]). Such a methodology is discussed in the following paragraphs, while validation of the approach is presented in Section V, for the PeWEC system.

We finish by noting that, with the representative response computed in (8), it is possible to perform, for a given interpolating frequency, the control synthesis procedure elucidated in Equation (3).

III. The PeWEC case

As discussed within Section I, among the available WECs, the PeWEC system has been chosen as a representative case study, due to its multi-degree-of-freedom (DoF) nature, comprehensive PTO conversion mechanism, and relevance of the mooring system for device station-keeping and alignment. A brief introduction to the PeWEC underlying working principle, mooring, and associated mechanical system, is conducted within the following subsections.

A. Working principle

The PeWEC is a floating offshore pendulum-based WEC, which harvests energy by means of the wave-induced pitch motion. Its working principle is outlined in Figure III-A. The PeWEC pitch motion, excited by the incoming wave, induces a pendulum rotation around its axis (ϵ), which is connected, by means of a gearbox, to a PTO system. Hull geometries and

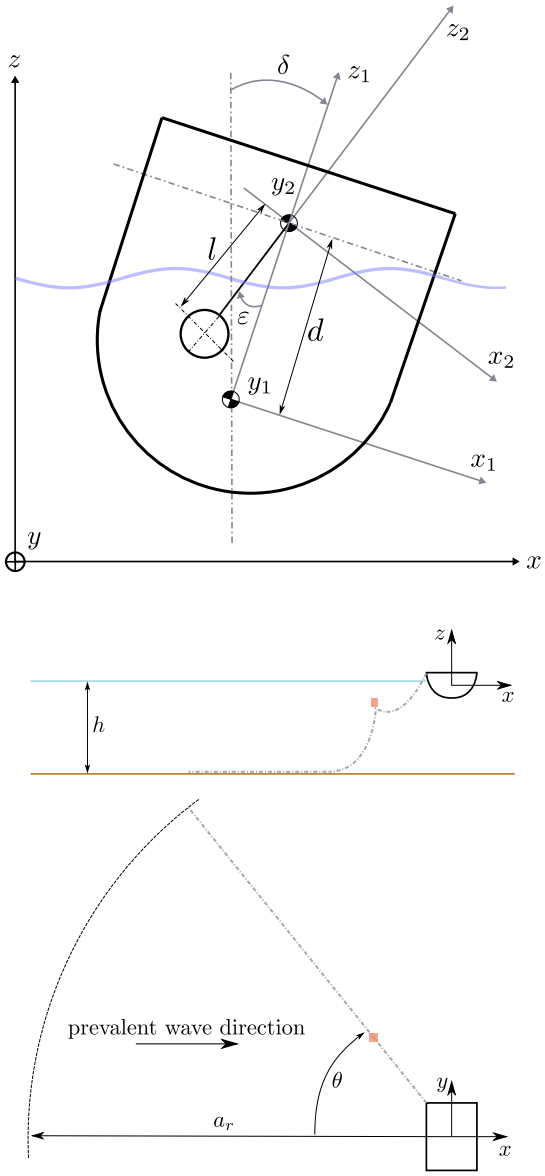

Fig. 4. The PeWEC system. Working principle is represented on the top, and the mooring layout is exposed on the bottom. The corresponding parameters are described in Table I.

inertial properties are the result of an optimisation algorithm, which evaluates the device performance and minimises a corresponding cost function (*i.e.* capex over productivity) on a specific site. In this case of study, the PeWEC device has been optimised on the environmental conditions of Pantelleria (Sicily, Italy), by adopting a genetic-based algorithm [32].

The PeWEC station-keeping problem is solved by adopting a symmetrical, spread mooring, formed by four catenary lines, which are effectively common within the wave energy field [33], [34]. Each line has a corresponding jumper attached, to reduce the vertical load on the device and, hence, minimise any undesired effects on the device response.

TABLE I
PEWEC PROPERTIES.

Property	Symbol	Unit	Value
PeWEC properties			
device mass	–	(kg)	$1.11 \cdot 10^6$
hull pitch inertial moment	I_y	(kg/m^3)	$3 \cdot 10^7$
device length	–	(m)	14.8
device width	–	(m)	22.5
pendulum mass	m	(kg)	$7.17 \cdot 10^4$
pendulum extent	d	(m)	2.44
pendulum length	l	(m)	2.40
Site & mooring properties			
site water depth	h	(m)	38
mooring anchor radius	a_r	(m)	175
mooring line length	–	(m)	190
mooring line angle	θ	(deg)	60
chain nominal diameter	–	(mm)	80
chain axial stiffness	–	(N)	$546 \cdot 10^6$
chain linear mass	–	(kg/m)	127
jumper net buoyancy	–	(kg)	4000

IV. NUMERICAL MODELS

In this section, the adopted numerical models for both WEC hydrodynamics, and mooring system, are outlined and discussed. Such models are considered for generation of representative input/output data, so as to characterise the device response as in Section II-B.

WEC hydrodynamics can be solved by means of several models. Commonly, the hydrodynamic problem is solved by means of a linear approach based on boundary element methods (BEMs) [35], which evaluates the hydrodynamic properties under the set of hypotheses generally known as potential flow theory [36]. Although the use of a solver with a higher degree of fidelity can potentially improve motion prediction, within operational range, linear theory provides a good trade-off between fidelity and computational time [35].

In contrast to hydrodynamic solvers, simplified mathematical models for mooring systems (such as static, or quasi-static solver), neglect inertial forces [17], which can play a fundamental role within the wave energy response, especially for catenary lines, where the restoring force is mainly a gravity-based action. Therefore, a numerical, dynamic, lumped-mass approach, is required to approximate the associated mooring response properly.

Although, as detailed within Section I, the case presented herein is based on the software OF, a significant part of the solvers commonly used is based on the same theory and methods. For instance, MOORDYN [37] and ANSYS AQWA [38] are open source and commercial software, respectively, based on a lumped-mass mooring solver. Nonetheless, even though OF is widely adopted, inclusion and simulation of a PTO system is not included as part of the software, and hence a general procedure to include any external action is proposed in Section IV-D.

A. Motion of a floating body

Following relatively standard assumptions (see e.g. [36]), Newton's law for a floating body can be written, $\forall t \in \Omega = [t_0, t_{end}] \subset \mathbb{R}^+$, as follows:

$$\mathcal{M}(t) = \mathcal{F}(t) - \mathcal{C}(t) - \mathcal{K}(t), \tag{9}$$

where $\{\mathcal{M}, \mathcal{F}, \mathcal{C}, \mathcal{K}\} : \Omega \to \mathbb{R}^6$, are the inertial, external, damping, and stiffness forces, respectively. The inertial term $\mathcal{M}$ is composed of the device inertial matrix and so-called infinite frequency added-mass. The device damping term, is defined in terms of the convolution integral of an associated impulse response function $I_{rf} : \Omega \to \mathbb{R}^{6\times6}$ [39], *i.e.*

$$\mathcal{C}(t) = \int_\Omega I_{rf}(\tau)\dot{q}(t-\tau)d\tau, \tag{10}$$

in which, the map $q : \Omega \to \mathbb{R}^6$ represents the floating body motion. The so-called "external" forces $\mathcal{F}$ can be separated as:

$$\mathcal{F}(t) = \mathcal{F}_w(t) + \mathcal{R}(t) + \mathcal{F}_m(t), \tag{11}$$

where $\{\mathcal{F}_w, \mathcal{R}, \mathcal{F}_m\}$ represent the wave 1^{st} order force, known as excitation force [40], the reaction of the PTO unit on the WEC hull, and the mooring force, respectively.

The hydrodynamic properties of the device (*i.e.* added mass, radiation damping, hydrostatic stiffness, and wave forces), are computed by means of BEM software. The BEM adopted within this study, which couples straightforwardly with the corresponding mooring solver, is ORCAWAVE (OW) [41].

B. Lumped-mass approach for mooring dynamics

OF solves the corresponding mooring system dynamics by adopting a lumped-mass approach [41]. The equation of each node can be written analogously to Equation (10) *i.e.*, $\forall t \in \Omega \subset \mathbb{R}^+$:

$$\mathcal{M}_m(t) = \mathcal{B}_m(t) - \mathcal{C}_m(t) - \mathcal{K}_m(t), \tag{12}$$

where $\{\mathcal{M}_m, \mathcal{C}_m, \mathcal{K}_m\} : \Omega \to \mathbb{R}^3$ are the inertial, damping, and stiffness forces associated with the mooring system, respectively. $\mathcal{B}_m : \Omega \to \mathbb{R}^3$ represents the external forces applied on the node, such as node weight and buoyancy load, hydrodynamic drag, and contact forces, among others.

C. Pendulum nonlinear mathematical model

The hull-pendulum interaction is discussed within this section. The pendulum equations are derived in a 3 DoF model and, hence, the effect of surge, heave, and pitch motion, are considered. Note that the presented mathematical model has been validated previously, see *e.g.* [42], [43]. The pendulum reaction on the hull $\mathcal{R} : \Omega \to \mathbb{R}^6$, $t \mapsto \mathcal{R}(t)$, can be written as

$$\begin{aligned}
\mathcal{R} &= [\mathcal{R}_{x_1}, 0, \mathcal{R}_{z_1}, 0, \mathcal{R}_\delta, 0,]^\intercal, \\
\mathcal{R}_{x_1} &= -md\cos(\delta)\ddot{\delta} - ml\cos(\delta+\epsilon)(\ddot{\delta}+\ddot{\epsilon}) \\
&+md\sin(\delta)\dot{\delta} - ml\sin(\delta+\epsilon)(\dot{\delta}+\dot{\epsilon})^2, \\
\mathcal{R}_{z_1} &= md\sin(\delta)\ddot{\delta} - ml\sin(\delta+\epsilon)(\ddot{\delta}+\ddot{\epsilon}) \\
&+md\cos(\delta)\dot{\delta} - ml\cos(\delta+\epsilon)(\dot{\delta}+\dot{\epsilon})^2, \\
\mathcal{R}_\delta &= \mathcal{F}_{\text{ctrl}} + \mathcal{R}_{x_1} d\cos(\delta) - \mathcal{R}_{z_1} d\sin(\delta),
\end{aligned} \tag{13}$$

where $\{m, l, d\} \subset \mathbb{R}^+$ represent the pendulum mass, pendulum length, and vertical extent between the pendulum fulcrum and the device CoG, respectively. Moreover, $\delta : \Omega \to \mathbb{R}$, $t \mapsto \delta(t)$ is the pitch motion, defined as the fifth-entry of the device motion vector q, and $\epsilon : \Omega \to \mathbb{R}$, $t \mapsto \epsilon(t)$ is the rotation of the PTO axis. Finally, $\mathcal{F}_{\text{ctrl}} : \Omega \to \mathbb{R}$, $t \mapsto \mathcal{F}_{\text{ctrl}}(t)$ is the control torque applied to the PTO axis. The relation between PeWEC pendulum rotation and its associated pitch motion can be described by means of the following equation:

$$\begin{aligned}&(I_y + ml^2)\ddot{\epsilon} - ml\cos(\delta+\epsilon)\ddot{x} + ml\sin(\delta+\epsilon)\ddot{z} + \\ &(I_y + ml^2 - mdl\cos(\epsilon))\ddot{\delta} - mdl\sin(\epsilon)\dot{\delta}^2 + \\ &mgl\sin(\delta+\epsilon) + \mathcal{F}_{\text{ctrl}} = 0,\end{aligned} \tag{14}$$

being $I_y \in \mathbb{R}^+$ the hull pitch inertial moment.

D. Pendulum integration via a dynamic library

This section proposes a general methodology for the integration of the PTO unit within OF, and its associated controller, to achieve a full high-fidelity numerical simulation, by following two procedures. In particular, according to [41], an external function can be included within OF either as a PYTHON code, or as a dynamic library (DLL in WINDOWS environment). Although the integration of a PYTHON code is facilitated by an embedded interface within OF (*i.e.* the code can be explicitly written in OF), in this study, the integration of the mechanical system is achieved by means of a DLL, for the reasons discussed below.

The dynamic library can be compiled leveraging C/C++ source code and, hence, facilitates the use of the embedded MATLAB [44] compiler, increasing significantly the potential of the tool, with the possibility of compiling SIMULINK or even SIMSCAPE models in C/C++ code. Despite the fact that the procedure to include the dynamic library, described herein, is linked to a specific WEC case (*i.e.* the PeWEC system), any other external force or interaction can be integrated in a OF model by following the same approach, hence providing a valuable tool for numerical simulation of a vast variety of moored WEC systems.

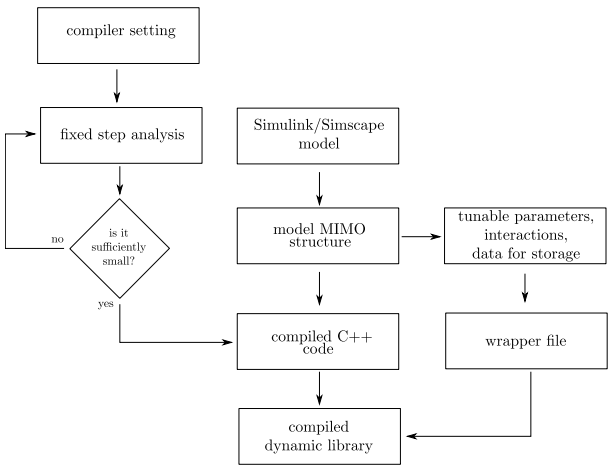

Fig. 5. Compiling process for the definition of OF external functions via a dynamic library.

The procedure followed to compile the dynamic library is outlined in Figure 5, and it can be summarised as follows:

- The model environment is set in order to compile the model as *generic real time* or *embedded real time* source code [44]. Although SIMULINK can solve the pendulum differential equation with a variable time step, a dynamic library solves the differential equation adopting a solver with a fixed time span, hence the time step needs to be set according to the underlying system dynamics.
- The model is included in a SIMULINK subsystem, specifying the associated input/output structure. Inputs and outputs of the subsystem are the information externally viewable by the C++ source code. Therefore, not only the information related to the hull-PTO interaction, but any useful variable (*i.e.* bearing forces for loss assessment), needs to be defined as output.
- The code can be now compiled by means of the SIMULINK compiler, and the solution generated, for example, via Visual Studio (directly connected with MATLAB/SIMULINK [44]). The source code contains the pendulum model that can be essentially used as a 'black-box' function.
- A wrapper file must be defined to ensure that OF is capable to see the model, and exchange the information with the dynamic library accordingly. All the significant variables previously defined in the Simulink input/output structure can be stored as outputs in the OF simulation file. SIMULINK parameters can be also defined as *tunable* parameters (*e.g.* control parameters), and it is possible to set and change these variables, among OF simulations, using the vessel tags.
- The DLL can be now compiled and imported in the OF model.

V. CONTROL SYNTHESIS FOR THE PEWEC

Although, within the PeWEC case, several control strategies have been applied [45], [46], [47], [48], the inclusion of the mooring forces in the control design procedure has not been explicitly considered.

Within the same approach proposed in Section II-A, the PeWEC control problem can be transcribed, under superposition assumptions, in terms of a generic LTI system, as reported in Figure 7 where, $\tilde{F}(\omega) : \mathbb{R} \to \mathbb{C}$ represents the Fourier transform of the total force applied by the hull onto the ϵ-axis (*i.e.* the pendulum axis), and where the elements of the set $\{G_p(\omega), I_u(\omega)\} : \mathbb{R}^+ \to \mathbb{C}$ represent pendulum and energy-maximising controller frequency response, respectively.

The identification of the map G_p, for the PeWEC case, is achieved by imposing a set of $N_j \in \mathbb{N}$ multisine input signals $\tilde{F}^j_{\text{ctrl}}$, as described in Section II-B. By applying this set of signals, and analogously to equation (8), it is straightforward to define the I/O empirical transfer function estimate for G_p as

$$G_p(\omega) = \sum_{j=1}^{N_j} \frac{1}{N_j} \frac{\tilde{F}^j_{\text{ctrl}}(\omega)}{\dot{E}^j(\omega)}, \tag{15}$$

where $\dot{E}^j$ denotes each output signal corresponding with the input $\tilde{\mathcal{F}}^j_{\text{ctrl}}$.

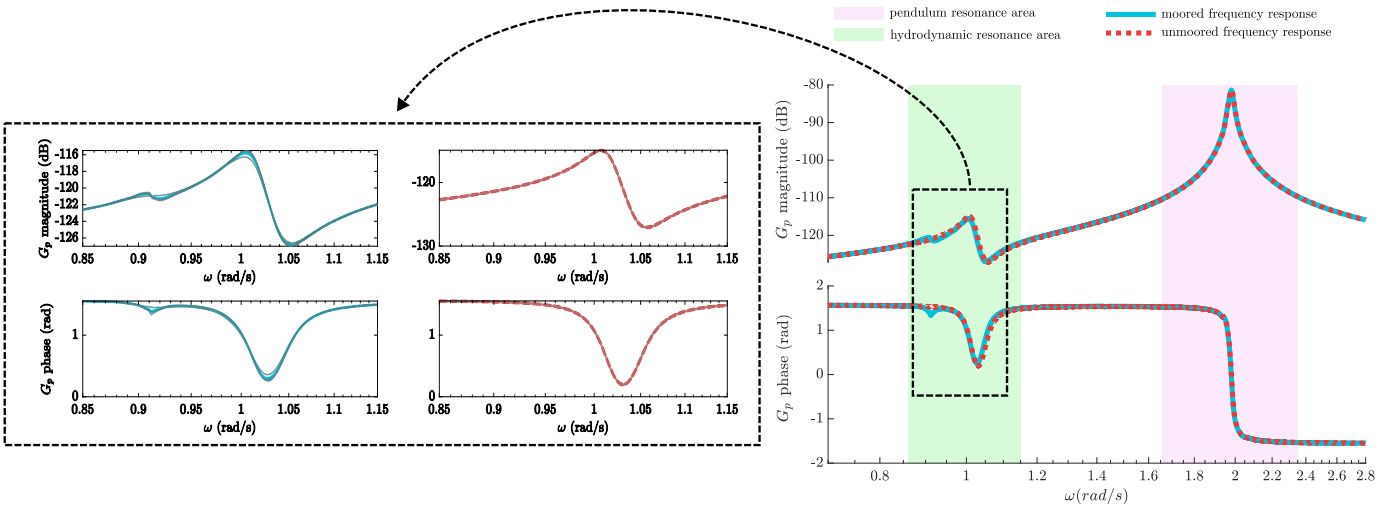

Fig. 6. On the left-hand side of the picture, the identified signals ($\tilde{F}^j_{\text{ctrl}}(\omega)/\dot{E}^j(\omega)$, in dark lines) are exposed and compared to the averaged values ($G_p(\omega)$). On the right-side hand side, the averaged frequency responses (G_p) for the moored and unmoored models are outlined.

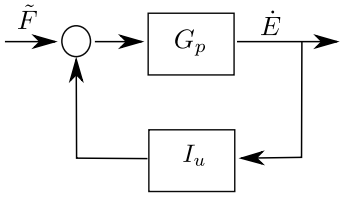

Fig. 7. LTI representation of the pendulum controlled system

The process described above is applied to both moored, and unmoored configurations, so as to evaluate the corresponding frequency response map for each case. In particular, this is exposed explicitly in Figure 6. It is possible to appreciate, in Figure 6, that the averaged map is representative of the system dynamics, with a slight variation as a function of the input exciting signal ($\tilde{F}^j_{\text{ctrl}}(\omega)$) for the moored map. Additionally, the pendulum dynamics is perfectly represented (see the unmoored frequency responses).

With the identified response (15), we proceed to synthesise an energy-maximising controller, following the impedance-matching theory presented in Section II. In particular, the structure of the feedback controller adopted in this paper, which is used to interpolate the optimal impedance-matching response as in (3), is:

$$I_u(\omega) = \frac{\alpha \jmath\omega}{\jmath\omega + \beta}, \tag{16}$$

with $\{\alpha, \beta\} \subset \mathbb{R}$. Note that the proposed controller structure is an alternative of the classic proportional-integral (PI) controller, well-known in the wave energy field. This particular structure is adopted for the intrinsic stability condition that can be guaranteed in the controller closed-loop form, taking advantage of the WEC dissipativity property [49].

Finally, by enforcing the interpolation condition in (3) in terms of the implementable structure (16), it is possible to define, for a given interpolating frequency $\omega_i \in \mathbb{R}$, the control parameters for (16) as follows:

$$\begin{aligned} \alpha_i(\omega_i) &= \Re\left(\frac{1}{G_p^*(\omega_i)}\right)\frac{\omega_i^2+\beta_i^2}{\omega_i^2}, \\ \beta_i(\omega_i) &= \Im\left(\frac{1}{G_p^*(\omega_i)}\right)\frac{\omega_i}{\Re\left(\frac{1}{G_p^*(\omega_i)}\right)}. \end{aligned} \tag{17}$$

VI. Analysis and Results

The effectiveness of the data-based modelling approach and associated control synthesis, carried out in Section V, is analysed in detail within this section. Note that, from now on, performance results are always evaluated within the high-fidelity numerical model described in Section IV. This clearly decouples the design process, based upon the data-based modelling approach presented, from the evaluation (benchmark) model.

We begin by testing the synthesised control performance in regular wave conditions, where the choice of the interpolating frequency for the impedance-matching process is clearly straightforward. Finally, to further test the proposed procedure in realistic sea-state conditions, the Pantelleria site is presented, and the performance assessment is carried out according to the main irregular sea states characterising such a location.

A. Power assessment under regular wave conditions

We begin by noting that, a variation between the moored and the unmoored pendulum map can be appreciated only in the hydrodynamic resonance area (see Figure 6), a representative set of frequencies (to characterise both the device responses and site conditions) is selected as interpolating frequencies.

Therefore, the associated control parameters (α and β), tuned accordingly for each wave condition, are reported in Figure 8, as function of the wave frequency. It is possible to notice that, clearly, a larger variation between moored and unmoored control parameters exists in the neighbourhood of

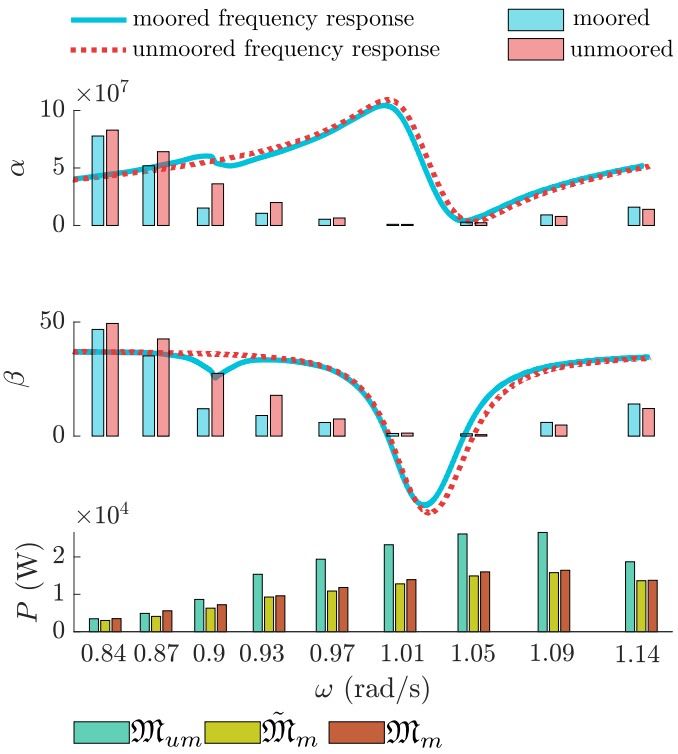

Fig. 8. Control parameters achieved by moored and unmoored empirical frequency responses.

$0.9\ rad/s$, which correlates with a larger variation in the associated frequency-response maps.

Figure 8 outlines the extracted mechanical power in regular wave conditions, defined as follows:

$$P = \overline{\mathcal{F}_{\text{ctrl}}(t)\dot{\epsilon}(t)}. \tag{18}$$

In addition, within Figure 8, $\{\tilde{\mathfrak{M}}_m, \mathfrak{M}_m\}$ refers to the high-fidelity numerical model of the fully moored PeWEC system, actuated with a controller synthesised by: a) ignoring the mooring dynamics when computing the associated data-based model (*i.e.* unmoored), and b) effectively including its behaviour, respectively. Moreover, to fully appreciate the importance and impact of the mooring inclusion within power assessment, $\mathfrak{M}_{um}$ is also included, which denotes the high-fidelity PeWEC model without considering the mooring system, actuated with a controller synthesised in the same condition (*i.e.* unmoored).

Note that the data-based synthesis approach proposed is effectively able to increase mechanical power absorption for all tested regular conditions, indicating that the modelling procedure provides a representative description of the overall system. Moreover, being the moored system significantly different from the unmoored device, it can happen that, for some frequencies (*e.g.* $0.87\ rad/s$), the moored device (controlled properly) is able to extract more mechanical power than its unmoored counterpart, effectively exploiting the mooring dynamics in a favourable fashion.

Figure 9 presents a phase-plane plot, which relates the pendulum axis rotation with its corresponding velocity, for a single input period in steady-state conditions. Given an exciting force

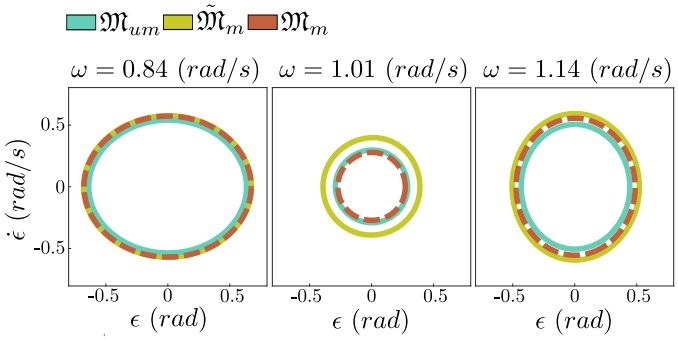

Fig. 9. ϵ phase plane diagram in regular conditions. When the system is in resonance condition, the pendulum motion is characterised by smaller motion (centre plot). Moreover, outside resonance, due to the reactive nature of the controller, the pendulum describes a larger trajectory (left and right plots).

defined in terms of a monochromatic input, *i.e.* $a_1 \sin(\omega t)$, and according to the impedance-matching conditions described in Section II-A (and implemented via the interpolation condition (15)), the pendulum velocity needs to be in-phase with the total excitation input and, hence, its associated position ϵ can be simply derived as

$$\dot{\epsilon}(t) = a_{\dot{\epsilon}} \sin(\omega t) \quad \rightarrow \quad \epsilon(t) = -\frac{a_{\dot{\epsilon}}}{\omega} \cos(\omega t), \tag{19}$$

where $a_{\dot{\epsilon}}$ is simply a scaled value of the exciting amplitude a_1 (see also equation (5)). Therefore, the resulting amplitude of the pendulum position is always smaller than its associated velocity for $\omega > 1$, and viceversa for $\omega < 1$, as it can be appreciated in the phase diagram of Figure 9. Furthermore, at resonance, *i.e.* $\omega \approx 1$, the trajectory of the pendulum on the phase diagram is effectively approximately described by a circle. Moreover, outside the resonance condition, reactive power is injected into the system, in order to enforce resonance with the incoming wave, and extract more mechanical energy. Clearly, the reactiveness of the control action causes an increment of the pendulum motion, which can be, based on technological constraints, an undesired effect.

We finish this section by noting that, within the moored configuration, not only the extracted power is always higher when including the mooring actions within the control synthesis, but the associated ϵ motion is actually always smaller, hence being even more beneficial from a technological perspective.

B. WEC performance on a wave scatter

This section extends the results presented in Section VI-A to the case of irregular wave conditions. In particular, within this study, the performance assessment is carried out according to the environmental conditions of the Pantelleria island (Sicily, Italy). Data has been downloaded from the ERA 5 hindcast online database [50]. Figure 10 shows the site energy scatter diagram (*i.e.* $J \cdot O_{cc}$) where, the power density (J) of a single wave, expressed in (kW/m), is [4]:

$$J = 0.49 T_e H_s^2, \tag{20}$$

with $\{T_e, H_s, O_{cc}\} \subset \mathbb{R}^+$ the energetic period, significant wave height, and wave occurrence, respectively. To analyse a representative set of environmental conditions, 15 waves are

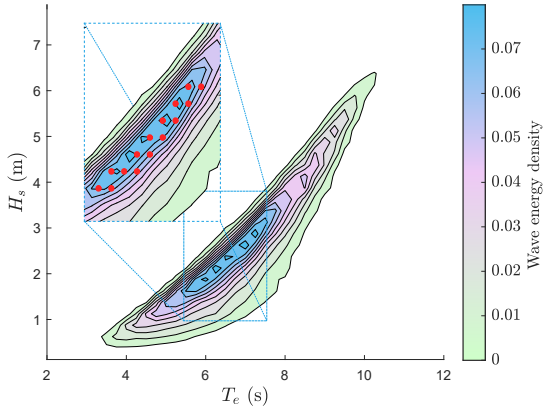

Fig. 10. Pantelleria energy density scatter.

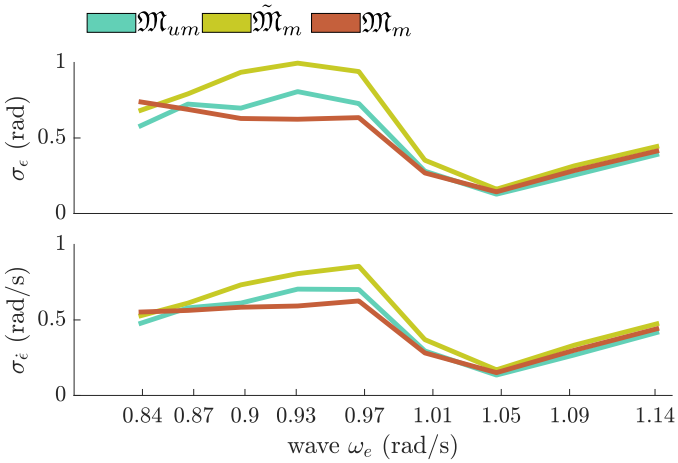

Fig. 11. Pendulum axis position and velocity root mean square variation.

chosen (Figure 10) and reported in Table II, being these waves the 15 most energetic waves on the Pantelleria scatter. The representation of the irregular sea states (listed in Table II) is achieved by means of the JONSWAP spectra [4].

TABLE II
WAVES LIST.

Wave number	T_e (s)	H_s (m)
1	6.25	2.125
2	7.25	2.875
3	7	2.625
4	6	1.875
5	6.5	2.375
6	6.75	2.375
7	6.75	2.625
8	7.5	3.125
9	5.75	1.875
10	6.5	2.125
11	5.75	1.625
12	5.5	1.625
13	6.25	1.875
14	7	2.875
15	7.25	3.125

By means of the impedance-matching technique, it is possible to compute the optimal control parameters, interpolating the I/O system impedance with the selected controller structure (as described in Section V). Unlike the regular wave case, where the choice of the interpolating frequency is effectively straightforward, an irregular sea state is characterised by a frequency bandwidth, and hence a suitable choice needs to be made. Within this study, the energetic period ω_e (Equation 21) is adopted as interpolating frequency for the identification of the control parameters, as performed in *e.g.* [51]. In particular,

$$\omega_e = 2\pi \frac{m_0}{m_{-1}}, \quad m_n = \int_{\mathbb{R}^+} \omega^n E(\omega) d\omega, \tag{21}$$

where $\{E(\omega), m_n\} \subset \mathbb{R}^+$ represent the variance density of the wave, and n-th order moment of the spectrum E, respectively. The simulation length is set to 1800 s, in order to consider a time span sufficiently large to be statistically consistent (see *e.g.* [52]).

The amplitude of the motion of the pendulum axis, and its associated velocity, is analysed within Figure 11. The analysis of the pendulum motion is presented by means of $\sigma_p \in \mathbb{R}^+$, being σ_p the root mean square of the variable p. Analogously to the case of the results presented in the phase-plane diagram for regular wave conditions (see Figure 9), within irregular wave condition, the same trend of pendulum motion can be appreciated. In particular, with effective knowledge of the mooring dynamics, the controller is able to maximise energy extraction accordingly, while presenting smaller motion requirements.

In Figure 12, the extracted mechanical power for each wave is presented, for all the analysed models. It is possible to appreciate that, since the moored system is significantly different from the unmoored one, and following the same trend exposed in regular wave conditions (see Section VI-A), the device tends to be more effective in low frequency waves, as can be appreciated in Figure 12 with the case of the wave 3. In addition, although the extracted power for waves 9, 11 and 12, which represent the higher frequencies $1.09, 1.14$ (rad/s), is slightly lower, the significant influence of the mooring system on both device dynamics, and associated harvested energy, can be clearly appreciated.

Although the mooring system is generally expected to have a negative impact on the overall performance of a WEC system (in terms of energy absorption), particular conditions do exist in which the effect of the station-keeping system is effectively positive in terms of the associated performance (the case of wave 3 in Figure 12). This is due to the fact that, as can be appreciated within Fig. 7, the magnitude associated with the response of the moored system is slightly larger that its unmoored counterpart in the frequency range where sea state 3 has significant energy components, hence producing an associated increase in energy performance.

Moreover, the results exposed in Figure 12 can be outlined and synthesised as exposed in Table III, being $\overline{P}$ the averaged extracted power. Note that a slight variation in the device dynamics, particularly for a resonating device, can influence significantly the final harvested energy. Moreover, the omission of the mooring dynamics within the control synthesis

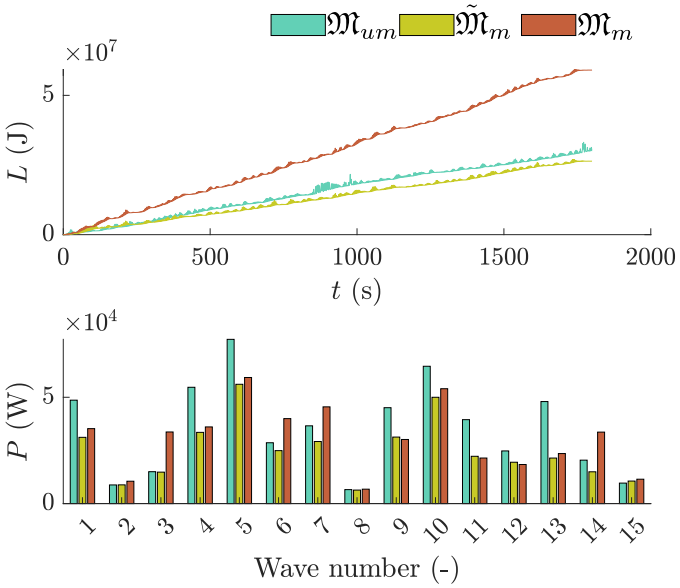

Fig. 12. Above, the harvested energy for wave 3 is outlined. Below, extracted power in irregular sea states for all the waves. In case of the wave 3 the moored system is able to harvest more energy than the unmoored one, since the system dynamics changes significantly.

procedure, for this case of study, can produce a decrease in final extracted power of up to 18%.

TABLE III
AVERAGED EXTRACTED MECHANICAL POWER.

model	$\overline{P}$ (kW)
$\mathfrak{M}_{um}$	35.2
$\tilde{\mathfrak{M}}_m$	25.0
$\mathfrak{M}_m$	30.6

We finish by noting that, a small influence on the system response map (see Figure 6), influences significantly the associated control synthesis and, accordingly, the device performance.

VII. Conclusions

The analysis of moorings systems for offshore WECs are is generally only included when addressing the station-keeping problem. This simplistic assumption is often driven by the underlying complexity behind including such effects within a tractable mathematical model. This study proposes a control-oriented data-based modelling procedure to include the mooring relevant dynamics, and perform a controller synthesis by means of the impedance-matching technique. The target data, used to compute such data-based control-oriented representation, is generated with a high-fidelity modelling solver, by using a specific set of representative persistenly exciting inputs.

As demonstrated within this paper by analysing the impact of the mooring itself on device dynamics, associated control synthesis, and resulting harvested energy, the influence of the station-keeping system within power assessment can be potentially large. In particular, the results in irregular wave conditions show a significant reduction of the extracted energy if the mooring is included in the power assessment analysis. Moreover, if the controller is synthesised with knowledge of the mooring dynamics, the resulting control action is considerably more effective, with improvements on final extracted mechanical power of up to 20%. In other words, reliable control synthesis for WEC systems needs to be performed by including mooring effects accordingly, such as performed within this paper with the proposed data-based approach.

Acknowledgments

Nicolás Faedo has received funding from the European Union's Horizon 2020 research and innovation programme under the Marie Sklodowska-Curie grant agreement No 101024372.

References

[1] IEA, IRENA, UNSD, WorldBank, and WHO, "Tracking sdg 7: The energy progress report," p. 268, 2022.
[2] T. W. Thorpe, "A brief review of wave energy a report produced for the uk department of trade and industry," 1999.
[3] A. Ilyas, S. A. Kashif, M. A. Saqib, and M. M. Asad, "Wave electrical energy systems: Implementation, challenges and environmental issues," *Renewable and Sustainable Energy Reviews*, vol. 40, pp. 260–268, 12 2014.
[4] WMO, *Guide to Wave Analysis and Forecasting*, 1998, vol. 1998.
[5] B. Czech and P. Bauer, "Wave energy converter concepts : Design challenges and classification," *IEEE Industrial Electronics Magazine*, vol. 6, pp. 4–16, 2012.
[6] M. A. Bhinder, M. Karimirad, S. Weller, Y. Debruyne, M. Guérinel, and W. Sheng, "Modelling mooring line non-linearities (material and geometric effects) for a wave energy converter using aqwa, sima and orcaflex," 2015, pp. 1–10.
[7] F. Depalo, S. Wang, S. Xu, and C. G. Soares, "Design and analysis of a mooring system for a wave energy converter," *Journal of Marine Science and Engineering*, vol. 9, 7 2021.
[8] Y. Mao, T. Wang, and M. Duan, "A dnn-based approach to predict dynamic mooring tensions for semi-submersible platform under a mooring line failure condition," *Ocean Engineering*, vol. 266, p. 112767, 12 2022.
[9] H. Wei, L. Xiao, M. Liu, and Y. Kou, "Data-driven model and key features based on supervised learning for truncation design of mooring and riser system," *Ocean Engineering*, vol. 224, p. 108743, 3 2021.
[10] J. Fitzgerald and L. Bergdahl, "Including moorings in the assessment of a generic offshore wave energy converter: A frequency domain approach," *Marine Structures*, vol. 21, pp. 23–46, 2008.
[11] F. Cerveira, N. Fonseca, and R. Pascoal, "Mooring system influence on the efficiency of wave energy converters," *International Journal of Marine Energy*, vol. 3-4, pp. 65–81, 12 2013.
[12] B. Paduano, E. Pasta, G. Papini, F. Carapellese, and G. Bracco, "Mooring influence on the productivity of a pitching wave energy converter," 2021, pp. 1–6.
[13] F. Niosi, L. Parrinello, B. Paduano, E. Pasta, F. Carapellese, and G. Bracco, "On the influence of mooring in wave energy converters productivity: the pewec case," 2021, pp. 1–6.
[14] E. Gubesch, N. Abdussamie, I. Penesis, and C. Chin, "Effects of mooring configurations on the hydrodynamic performance of a floating offshore oscillating water column wave energy converter," *Renewable and Sustainable Energy Reviews*, vol. 166, p. 112643, 9 2022.
[15] N. Faedo, E. Pasta, F. Carapellese, V. Orlando, D. Pizzirusso, D. Basile, and S. A. Sirigu, "Energy-maximising experimental control synthesis via impedance-matching for a multi degree-of-freedom wave energy converter," *IFAC-PapersOnLine*, vol. 55, pp. 345–350, 2022, 14th IFAC Conference on Control Applications in Marine Systems, Robotics, and Vehicles CAMS 2022.
[16] N. Faedo, F. Carapellese, E. Pasta, and G. Mattiazzo, "On the principle of impedance-matching for underactuated wave energy harvesting systems," *Applied Ocean Research*, vol. 118, p. 102958, 1 2022.
[17] J. Davidson and J. V. Ringwood, "Mathematical modelling of mooring systems for wave energy converters - a review," *Energies*, vol. 10, 2017.

[18] N. Pozzi, "Numerical modeling and experimental testing of a pendulum wave energy converter (pewec)," 2018.

[19] B. Paduano, F. Carapellese, E. Pasta, N. Faedo, and G. Mattiazzo, "Optimal controller tuning for a nonlinear moored wave energy converter via non-parametric frequency-domain techniques," 2022.

[20] J. V. Ringwood, A. Merigaud, N. Faedo, and F. Fusco, "An analytical and numerical sensitivity and robustness analysis of wave energy control systems," *IEEE Transactions on Control Systems Technology*, pp. 1–12, 4 2019.

[21] N. Faedo, D. García-Violini, Y. Peña-Sanchez, and J. V. Ringwood, "Optimisation- vs. non-optimisation-based energy-maximising control for wave energy converters: A case study," 2020, pp. 843–848.

[22] Andrea, P. V. G. S., P. Sonja, X. I. Z. Mario, and Boccia, "Direct optimal control and model predictive control," pp. 263–382, 2017. [Online]. Available: https://doi.org/10.1007/978-3-319-60771-9_3

[23] A. Karthikeyan, M. Previsic, J. Scruggs, and A. Chertok, "Non-linear model predictive control of wave energy converters with realistic power take-off configurations and loss model," 2019, pp. 270–277.

[24] R. Genest and J. V. Ringwood, "Receding horizon pseudospectral control for energy maximization with application to wave energy devices," *IEEE Transactions on Control Systems Technology*, vol. 25, pp. 29–38, 2017.

[25] J. V. Ringwood, A. Merigaud, N. Faedo, and F. Fusco, "Wave energy control systems: Robustness issues," 2018.

[26] J. T. Scruggs, S. M. Lattanzio, A. A. Taflanidis, and I. L. Cassidy, "Optimal causal control of a wave energy converter in a random sea," *Applied Ocean Research*, vol. 42, pp. 1–15, 2013.

[27] T. L. Floyd and E. Pownell, *Principles of electric circuits.* PEARSON INDIA, 2000.

[28] J. Davidson, S. Giorgi, and J. V. Ringwood, "Linear parametric hydrodynamic models for ocean wave energy converters identified from numerical wave tank experiments," *Ocean Engineering*, vol. 103, pp. 31–39, 2015.

[29] R. Pintelon and J. Schoukens, *System Identification: A Frequency Domain Approach*. Wiley, 2004.

[30] J. Schoukens, R. Pintelon, E. V. D. Ouderaa, and J. Renneboog, "Survey of excitation signals for fft based signal analyzers," *IEEE Transactions on Instrumentation and Measurement*, vol. 37, pp. 342–352, 1988.

[31] R. Pintelon and J. Schoukens, *System Identification: A Frequency Domain Approach, Second Edition*, 2012, cited by: 996. [Online]. Available: https://www.scopus.com/inward/record.uri?eid=2-s2.0-84891585276&doi=10.1002%2f9781118287422&partnerID=40&md5=c4ed2cc5a43112831897b48a659c66e3

[32] S. A. Sirigu, L. Foglietta, G. Giorgi, M. Bonfanti, G. Cervelli, G. Bracco, and G. Mattiazzo, "Techno-economic optimisation for a wave energy converter via genetic algorithm," *Journal of Marine Science and Engineering*, vol. 8, 2020.

[33] R. E. Harris, L. Johanning, J. Wolfram, and M. Frsa, "Mooring systems for wave energy converters: A review of design issues and choices."

[34] D. Qiao, R. Haider, J. Yan, D. Ning, and B. Li, "Review of wave energy converter and design of mooring system," *Sustainability (Switzerland)*, vol. 12, pp. 1–31, 2020.

[35] M. Penalba, G. Giorgi, and J. V. Ringwood, "Mathematical modelling of wave energy converters: a review of nonlinear approaches," *Renewable and Sustainable Energy Reviews*, vol. 78, pp. 1188–1207, 2017.

[36] O. Faltinsen, *Sea Loads on Ships and Offshore Structures*. Cambridge University Press, 1993.

[37] M. Hall, "Moordyn user ' s guide," 2015.

[38] ANSYS, "Aqwa theory manual," p. 174, 2013.

[39] W. E. Cummins, "The impulse response function and ship motions," *Schiffstechnik*, vol. 9 (Heft 47, pp. 101–109, 1962.

[40] J. M. J. Journee and W. W. Massie, *Offshore Hydromechanics*, 1st ed. Delft University of Technology, 2001.

[41] Orcina, "Orcaflex - documentation, 10.1b edition," 2020.

[42] N. Pozzi, M. Bonfanti, and G. Mattiazzo, "Mathematical modeling and scaling of the friction losses of a mechanical gyroscope," *International Journal of Applied Mechanics*, vol. 10, 2018.

[43] N. Pozzi, G. Bracco, B. Passione, S. A. Sirigu, and G. Mattiazzo, "Pewec: Experimental validation of wave to pto numerical model," *Ocean Engineering*, vol. 167, pp. 114–129, 11 2018.

[44] Mathworks, *MATLAB (R2019b)*, 9th ed. The MathWorks Inc., 2019.

[45] F. Carapellese, E. Pasta, B. Paduano, N. Faedo, and G. Mattiazzo, "Intuitive lti energy-maximising control for multi-degree of freedom wave energy converters: the pewec case," *Ocean Engineering*, 2022.

[46] E. Pasta, F. Carapellese, and G. Mattiazzo, "Deep neural network trained to mimic nonlinear economic model predictive control: an application to a pendulum wave energy converter." IEEE, 2021, pp. 295–300.

[47] D. G. Gioia, E. Pasta, P. Brandimarte, and G. Mattiazzo, "Data-driven control of a pendulum wave energy converter: A gaussian process regression approach," *Ocean Engineering*, vol. 253, p. 111191, 2022.

[48] N. Pozzi, G. Bracco, B. Passione, A. S. Sergej, G. Vissio, G. Mattiazzo, and G. Sannino, "Wave tank testing of a pendulum wave energy converter 1:12 scale model," *International Journal of Applied Mechanics*, vol. 9, 2017.

[49] N. Faedo, Y. Peña-Sanchez, F. Carapellese, G. Mattiazzo, and J. V. Ringwood, "Lmi-based passivation of lti systems with application to marine structures," *IET Renewable Power Generation*, vol. 15, pp. 3424–3433, 10 2021, https://doi.org/10.1049/rpg2.12286.

[50] H. Hersbach, B. Bell, P. Berrisford, and et al., "The era5 global reanalysis," *Quarterly Journal of the Royal Meteorological Society*, vol. 146, pp. 1999–2049, 2020.

[51] N. Faedo, G. Giorgi, J. V. Ringwood, and G. Mattiazzo, "Optimal control of wave energy systems considering nonlinear froude–krylov effects: control-oriented modelling and moment-based control," *Nonlinear Dynamics*, vol. 109, pp. 1777–1804, 2022.

[52] A. Merigaud, "A harmonic balance framework for the numerical simulation of non-linear wave energy converter models in random seas," 2018.